CHAPTER 2

MATHEMATICAL ANALYSIS OF ONE DIMENSIONAL UNSTEADY FREE CONVECTIVE MHD NANOFLUID FLOW WITH HEAT TRANSFER

Content of this chapter is published in Journal of Nigerian Mathematical Society **(Elsevier)**, 34 (2015) 303–317.

Chapter 2

MATHEMATICAL ANALYSIS OF ONE DIMENSIONAL UNSTEADY FREE CONVECTIVE MHD NANOFLUID FLOW WITH HEAT TRANSFER

Analytic expression for unsteady hydromagnetic boundary layer flow past an oscillating vertical plate in optically thick nanofluid in presence of thermal radiation and uniform transverse magnetic field is obtained. The Rosseland diffusion flux model is adopted to simulate thermal radiation effects. The momentum and energy conservation equations are made dimensionless, and analytic solution is obtained using the Laplace transform. The expressions for velocity and temperature are obtained and plotted graphically.

2.1 Introduction of the problem

Working fluids have great demands placed upon them in terms of increasing or decreasing energy release to systems, and their influences depend on thermal conductivity, heat capacity and other physical properties in modern thermal and manufacturing processes. Potential for heat transfer in the high-tech applications such as microelectronics, data centres and micro-channels have attracted the most attentions. Conventional heat transfer fluids such as ethylene glycol, water, pumping oil, etc., do not possess sufficient capability for cooling applications due to their poor thermal performance. A low thermal conductivity is one of the most remarkable parameters that can limit the heat transfer performance. Adding solid particles to these fluids could enhance their thermal performance.

This is one of the most modern and appropriate methods for increasing the coefficient of heat transfer. However, still suspensions with micrometre or larger size particles are not efficient choice for such applications. Therefore, development of highly efficient heat transfer fluids for solving the drawback of conventional fluids has become one of the most important priorities in the cooling industries.

A mixture of nanoparticles and base fluid is designated as nanofluids. In nanoparticles, due to the increase of surface area to the volume, some physical properties such as thermal, electrical, mechanical, optical and magnetic properties of the materials can be changed significantly. The most important point is that nano structured materials exhibit different and unique properties as compared to the bulk materials with the same compositions. Experimental studies have displayed that with 1–5% volume of solid metallic or metallic oxide particles, the effective thermal conductivity of the resulting mixture can be increased by 20% compared to that of the base fluid.

The study of magnetohydrodynamics flow and heat transfer has received considerable attention in recent years due to its essential applications in engineering and technology such as MHD generators, pumps, plasma studies, bearings, nuclear reactors and geothermal energy extractions. Interaction between the electrically conducting fluid and a magnetic field is used as a control mechanism in material manufacturing industry, as the convection currents are suppressed by Lorentz force which is produced by the magnetic field. Thermal Radiation transfer is also essential in nuclear power plants, gas turbines and various propulsion devices for aircrafts, missiles, satellites and space vehicles.

The gravity-driven convective heat transfer is a vital phenomenon in the cooling mechanism of many engineering systems like the electronics industry, solar collectors and cooling systems for nuclear reactors because of its minimum cost, low noise, smaller size and reliability. Motsumi and Makinde [46] studied the problem of MHD with convective boundary layer flow and heat transfer characteristics over a vertical plate. The MHD boundary layer flow over a vertical stretching/shrinking sheet in a nanofluid was investigated by Makinde et al. [44] and Das et al. [10]. Sheikholeslami et al. [106] discussed effects of thermal radiation on magnetohydrodynamics nanofluid flow.

Chapter 2

The study of gravity-driven MHD flow of an optically thick fluid past an infinite vertical plate is considered very essential in understanding the behaviour of the performance of fluid motion in several applications. The problem of gravity-driven convection in a regular fluid past a vertical plate is a classical problem solved by Ostrach [54].

Convective flows with radiation are also encountered in many industrial processes such as heating and cooling of chambers, energy processes, evaporation from large reservoirs, solar power technology and space vehicle re-entry. Thermal radiation effects of an optically thin gray gas bounded by a stationary vertical plate are investigated by England and Emery [13]. The effective thermal conductivity of the nanofluid given by Hamilton and Crosser was followed by Kakac and Pramuanjaroenkij [26], and Oztop and Abu-Nada [56].

2.2 Novelty of the Problem

The aim of this chapter is to study the hydromagnetic gravity-driven convective boundary layer flow of nanofluids past an oscillating vertical plate in presence of a uniform transverse magnetic field and thermal radiation. The fluid flow is assumed to be induced by motion of the plate. Water based nanofluids containing nanoparticles of copper (Cu) and Silver (Ag) have been considered in the present work. The governing equations are solved analytically.

2.3 Mathematical formulation of the Problem

As in Figure 2.1, the flow is confined to $y' > 0$, where y' is the coordinate measured in the normal direction to the plate. The fluid is assumed to be electrically conducting with a uniform magnetic field B, applied in a direction perpendicular to the plate. Induced magnetic field produced by the fluid motion is negligible in comparison with the applied one as the magnetic Reynolds number is small enough to neglect the effects of induced magnetic field.

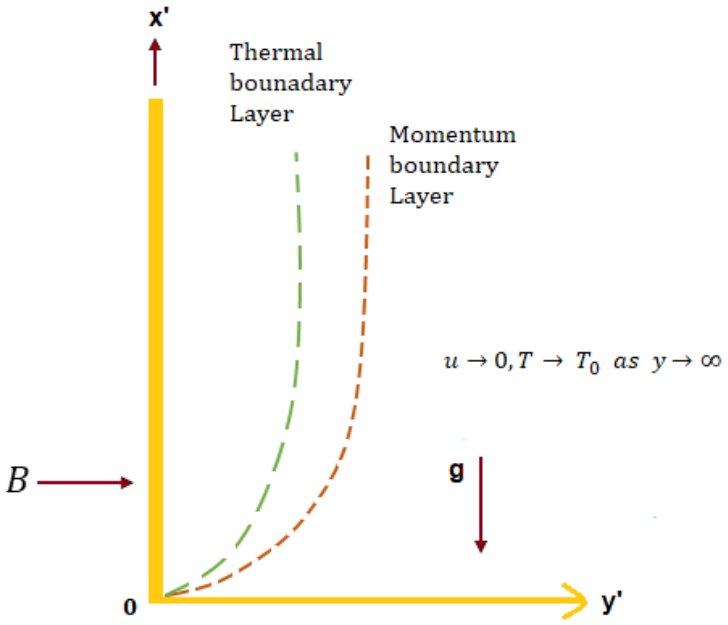

Figure 2.1: Physical Sketch of the Problem

At time $t' = 0$, the plate is at rest with the constant ambient temperature T_0. At time $t' > 0$, the plate begins to oscillate in its own plane according to $u_0 \sin \omega' t'$, where u_0 is amplitude of the plate oscillations and the temperature of the plate is raised or lowered to T_w. As nanofluid is optically thick, radiative flux can be approximated using Rosseland approximation [40]. It is also assumed that a radiative heat flux q_r is applied in the normal direction to the plate. A medium is said to be optically thick if radiation exchange occurs only among neighbouring volume elements. This is diffusion limit, in which the governing radiative transport equations are differential equations. The fluid is a water based nanofluid containing copper or silver as nanoparticles. It is further assumed that the base fluid and the suspended nanoparticles are in thermal equilibrium and density is linearly dependent on temperature buoyancy forces.

Under these assumptions, the momentum and energy equations in the presence of thermal radiation and magnetic field past an oscillating vertical plate can be expressed as

$$\rho_{nf}\frac{\partial u'}{\partial t'} = \mu_{nf}\frac{\partial^2 u'}{\partial y'^2} + g(\rho\beta)_{nf}(T' - T_0) - \sigma_{nf}B^2u' \tag{2.1}$$

$$\left(\rho c_p\right)_{nf}\frac{\partial T'}{\partial t'} = k_{nf}\frac{\partial^2 T'}{\partial y'^2} - \frac{\partial q_r}{\partial y'} \tag{2.2}$$

where

$$\rho_{nf} = (1 - \emptyset)\rho_f + \emptyset\rho_s \tag{2.3}$$

$$\mu_{nf} = \frac{\mu_f}{(1-\emptyset)^{2.5}} \tag{2.4}$$

$$\sigma_{nf} = \sigma_f[1 + \frac{3(\sigma-1)\emptyset}{(\sigma+2)-(\sigma-1)\emptyset}], \sigma = \frac{\sigma_s}{\sigma_f} \tag{2.5}$$

$$(\rho\beta)_{nf} = (1 - \emptyset)(\rho\beta)_f + \emptyset(\rho\beta)_s \tag{2.6}$$

$$k_{nf} = k_f[1 - 3\frac{\emptyset(k_f - k_s)}{2k_f + k_s + \emptyset(k_f - k_s)}] \tag{2.7}$$

$$\left(\rho c_p\right)_{nf} = (1 - \emptyset)(\rho c_p)_f + \emptyset(\rho c_p)_s \tag{2.8}$$

$$q_r = -\frac{4\sigma^*}{3k^*}\frac{\partial T'^4}{\partial y'} \tag{2.9}$$

The thermo-physical properties of the base fluid (water) and different nanoparticles are given in Table 1.1.

Considering temperature difference within the flow to be sufficiently small, using Taylor's series and neglecting higher terms, Equation (2.9) becomes

$$q_r = -\frac{4\sigma^*}{3k^*}\frac{\partial(4T_0^{\,3}T' - 3T_0^{\,4})}{\partial y'} \tag{2.10}$$

Using Equation (2.10) in (2.2)

$$\left(\rho c_p\right)_{nf}\frac{\partial T'}{\partial t'} = \left(k_{nf} + \frac{16\sigma^*T_0^{\,3}}{3k^*}\right)\frac{\partial^2 T'}{\partial y'^2}, \tag{2.11}$$

The initial and boundary conditions are

$t' = 0\,,\ u' = 0,\ T' = T_0 \quad \text{for } y' \geq 0$

$t' > 0\,,\ u' = u_0 \sin \omega' t'\,,\ T' = T_w \quad \text{for } y' = 0$

$t' > 0\,,\ u' \to 0,\ T' \to T_0 \ \text{ as } \ y' \to \infty$ (2.12)

Introducing non dimensional variables

$y = \frac{u_0 y'}{v_f}, t = \frac{{u_0}^2 t'}{v_f}, u = \frac{u'}{u_0}, \theta = \frac{T' - T_0}{T_w - T_0}, \omega = \frac{v_f \omega'}{{u_0}^2},$ (2.13)

(2.1) and (2.11) become

$\frac{\partial \mathrm{u}}{\partial \mathrm{t}} = \mathrm{a}_1 \frac{\partial^2 \mathrm{u}}{\partial \mathrm{y}^2} + \mathrm{G_r a_2 \theta} - M \mathrm{a_3 u}$ (2.14)

$\frac{\partial \theta}{\partial \mathrm{t}} = \mathrm{a}_4 \frac{\partial^2 \theta}{\partial \mathrm{y}^2}$ (2.15)

where

$b_0 = 1 - \emptyset$ (2.16)

$b_1 = (b_0 + \emptyset \frac{\rho_s}{\rho_f}),$ (2.17)

$b_2 = (b_0 + \emptyset \frac{(\rho\beta)_s}{(\rho\beta)_f}),$ (2.18)

$b_3 = (b_0 + \emptyset \frac{(\rho c_p)_s}{(\rho c_p)_f}),$ (2.19)

$b_4 = \frac{k_{nf}}{k_f},$ (2.20)

$b_5 = \frac{\sigma_{nf}}{\sigma_f},$ (2.21)

$$b_6 = \frac{b_4}{b_3}, \tag{2.22}$$

$$a_1 = \frac{1}{{b_0}^{2.5} b_1}, \tag{2.23}$$

$$a_2 = \frac{b_2}{b_1}, \tag{2.24}$$

$$a_3 = \frac{b_5}{b_1}, \tag{2.25}$$

$$a_4 = \frac{b_4 + Nr}{b_3 pr}, \tag{2.26}$$

$$M = \frac{\sigma_f B^2 v_f}{\rho_f {u_0}^2} \tag{2.27}$$

$$Nr = \frac{16\sigma^* {T_0}^3}{3k^* k_f} \tag{2.28}$$

$$Pr = \frac{\mu_f \left(\rho c_p\right)_f}{\rho_f k_f}, \tag{2.29}$$

$$Gr = \frac{g\beta_f (T_w - T_0) v_f}{{u_0}^3} \tag{2.30}$$

The corresponding initial and boundary conditions are

$t = 0,\ u = 0,\ \theta = 0 \quad$ for $y \geq 0$

$t > 0,\ u = \sin \omega t,\ \theta = 1 \quad$ for $y = 0$

$u \to 0,\ \theta \to 0 \quad$ as $y \to \infty$ (2.31)

2.4 Solution of the problem

Taking Laplace transform of equation (2.14),

$$\bar{u} = \frac{i}{2} F_1(y, s) - \frac{i}{2} F_2(y, s) - c_6 F_3(y, s) + c_6 F_4(y, s) + c_6 F_5(y, s) - c_6 F_6(y, s) \tag{2.32}$$

Taking Laplace transform of equation (2.15),

$$\bar{\theta} = \frac{1}{s} e^{-y\sqrt{s/a_4}} \tag{2.33}$$

Where

$$F_1(y,s) = \frac{e^{-y\sqrt{\frac{(s+c_1)}{a_1}}}}{(s+i\omega)} \tag{2.34}$$

$$F_2(y,s) = \frac{e^{-y\sqrt{\frac{(s+c_1)}{a_1}}}}{(s-i\omega)} \tag{2.35}$$

$$F_3(y,s) = \frac{e^{-y\sqrt{\frac{(s+c_1)}{a_1}}}}{s} \tag{2.36}$$

$$F_4(y,s) = \frac{e^{-y\sqrt{\frac{(s+c_1)}{a_1}}}}{(s-c_4)} \tag{2.37}$$

$$F_5(y,s) = \frac{e^{-y\sqrt{s/a_4}}}{s} \tag{2.38}$$

$$F_6(y,s) = \frac{e^{-y\sqrt{s/a_4}}}{(s-c_4)} \tag{2.39}$$

Taking inverse Laplace transform of equations (2.32 - 2.33),

$$u(y,t) = \frac{i}{2} f_1(y,t) - \frac{i}{2} f_2(y,t) - c_6 f_3(y,t) + c_6 f_4(y,t) + c_6 f_5(y,t) - c_6 f_6(y,t) \tag{2.40}$$

$$\theta(y,t) = \operatorname{erfc}\left(\frac{y\sqrt{1/a_4}}{2\sqrt{t}}\right) \tag{2.41}$$

Here erfc is Complementary error function.

where,

$$f_1(y,t) = \frac{e^{-i\omega t}}{2}\left[e^{-y\sqrt{\frac{1}{a_1}(c_1-i\omega)}}\ \text{erfc}\left(\frac{y}{2\sqrt{a_1 t}} - \sqrt{(c_1-i\omega)t}\right) + e^{y\sqrt{\frac{1}{a_1}(c_1-i\omega)}}\ \text{erfc}\left(\frac{y}{2\sqrt{a_1 t}} + \sqrt{(c_1-i\omega)t}\right)\right] \quad (2.42)$$

$$f_2(y,t) = \frac{e^{i\omega t}}{2}\left[e^{-y\sqrt{\frac{1}{a_1}(c_1+i\omega)}}\ \text{erfc}\left(\frac{y}{2\sqrt{a_1 t}} - \sqrt{(c_1+i\omega)t}\right) + e^{y\sqrt{\frac{1}{a_1}(c_1+i\omega)}}\ \text{erfc}\left(\frac{y}{2\sqrt{a_1 t}} + \sqrt{(c_1+i\omega)t}\right)\right] \quad (2.43)$$

$$f_3(y,t) = \frac{1}{2}\left[e^{-y\sqrt{\frac{c_1}{a_1}}}\ \text{erfc}\left(\frac{y}{2\sqrt{a_1 t}} - \sqrt{c_1 t}\right) + e^{-y\sqrt{\frac{c_1}{a_1}}}\ \text{erfc}\left(\frac{y}{2\sqrt{a_1 t}} + \sqrt{c_1 t}\right)\right] \quad (2.44)$$

$$f_4(y,t) = \frac{e^{c_4 t}}{2}\left[e^{-y\sqrt{\frac{1}{a_1}(c_1+c_4)}}\ \text{erfc}\left(\frac{y}{2\sqrt{a_1 t}} - \sqrt{(c_1+c_4)t}\right) + e^{y\sqrt{\frac{1}{a_1}(c_1+c_4)}}\ \text{erfc}\left(\frac{y}{2\sqrt{a_1 t}} + \sqrt{(c_1+c_4)t}\right)\right] \quad (2.45)$$

$$f_5(y,t) = \text{erfc}\left(\frac{y}{2\sqrt{a_4 t}}\right) \quad (2.46)$$

$$f_6(y,t) = \frac{e^{c_4 t}}{2}\left[e^{-y\sqrt{\frac{c_4}{a_4}}}\ \text{erfc}\left(\frac{y}{2\sqrt{a_4 t}} - \sqrt{c_4 t}\right) + e^{y\sqrt{\frac{c_4}{a_4}}}\ \text{erfc}\left(\frac{y}{2\sqrt{a_4 t}} + \sqrt{c_4 t}\right)\right] \quad (2.47)$$

$$c_1 = M a_3 \quad (2.48)$$

$$c_2 = G_r a_2 \quad (2.49)$$

$$c_3 = \frac{a_1}{a_4} - 1 \quad (2.50)$$

$$c_4 = \frac{c_1}{c_3} \quad (2.51)$$

$$c_5 = \frac{c_2}{c_3} \quad (2.52)$$

$$c_6 = \frac{c_5}{c_4} \quad (2.53)$$

2.5 Nusselt Number:

From the equation (2.41), Nusselt number Nu can be written as

$$N_u = -\sqrt{\frac{1}{a_4\,\pi\,t}} \quad (2.54)$$

2.6 Skin Friction:

From the equations (2.40), skin friction τ can be written as

$$\tau(y,t) = \frac{i}{2}h_1(t) - \frac{i}{2}h_2(t) - \mathrm{c}_6\, h_3(t) + \mathrm{c}_6\, h_4(t) + \mathrm{c}_6\, h_5(t) - \mathrm{c}_6\, h_6(t) \tag{2.55}$$

Where

$$h_1(t) = e^{-i\omega t}\sqrt{\frac{c_1 - i\omega}{a_1}}\,\mathrm{erf}\left(\sqrt{(c_1 - i\omega)t}\right) + \frac{e^{-c_1 t}}{\sqrt{\pi a_1 t}} \tag{2.56}$$

$$h_2(t) = e^{i\omega t}\sqrt{\frac{c_1 + i\omega}{a_1}}\,\mathrm{erf}\left(\sqrt{(c_1 + i\omega)t}\right) + \frac{e^{-c_1 t}}{\sqrt{\pi a_1 t}} \tag{2.57}$$

$$h_3(t) = -\sqrt{\frac{c_1}{a_1}}\,\mathrm{erf}(\sqrt{c_1 t}) + \frac{e^{-c_1 t}}{\sqrt{\pi a_1 t}} \tag{2.58}$$

$$h_4(t) = e^{\mathrm{c}_4 t}\sqrt{\frac{\mathrm{c}_4 + \mathrm{c}_1}{\mathrm{a}_1}}\,\mathrm{erf}\left(\sqrt{(\mathrm{c}_4 + \mathrm{c}_1)t}\right) + \frac{e^{-c_1 t}}{\sqrt{\pi a_1 t}} \tag{2.59}$$

$$h_5(t) = \sqrt{\frac{1}{a_4\,\pi\, t}} \tag{2.60}$$

$$h_6(t) = -e^{\mathrm{c}_4 t}\sqrt{\frac{\mathrm{c}_4}{\mathrm{a}_4}}\,\mathrm{erf}(\sqrt{\mathrm{c}_4 t}) + \frac{1}{\sqrt{\pi a_4 t}} \tag{2.61}$$

2.7 Results and Discussion:

Obtained numerical results are elucidated with the help of graphical illustrations to get a clear insight on the physics of the problem. Numerical results for velocity profile as well as temperature profile are presented for different values of various parameters, involved in dimensionless equations.

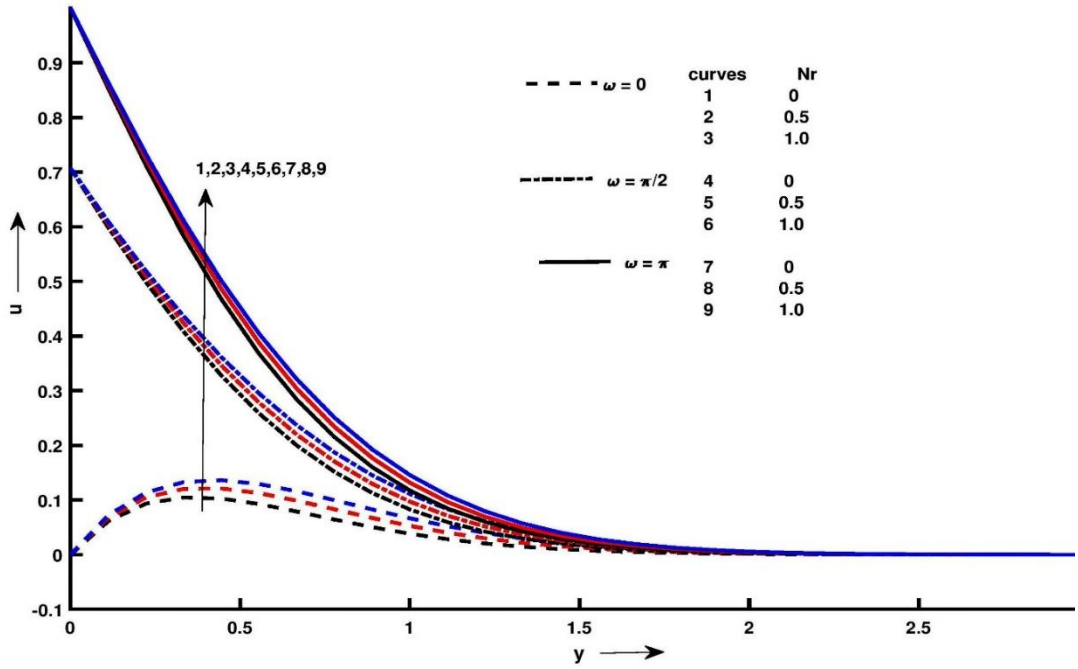

Figure 2.2: Velocity profile for y and Nr at $t = 0.5,\ M = 3, Gr = 5,$ $\emptyset = 0.03,\ Pr = 6.2$

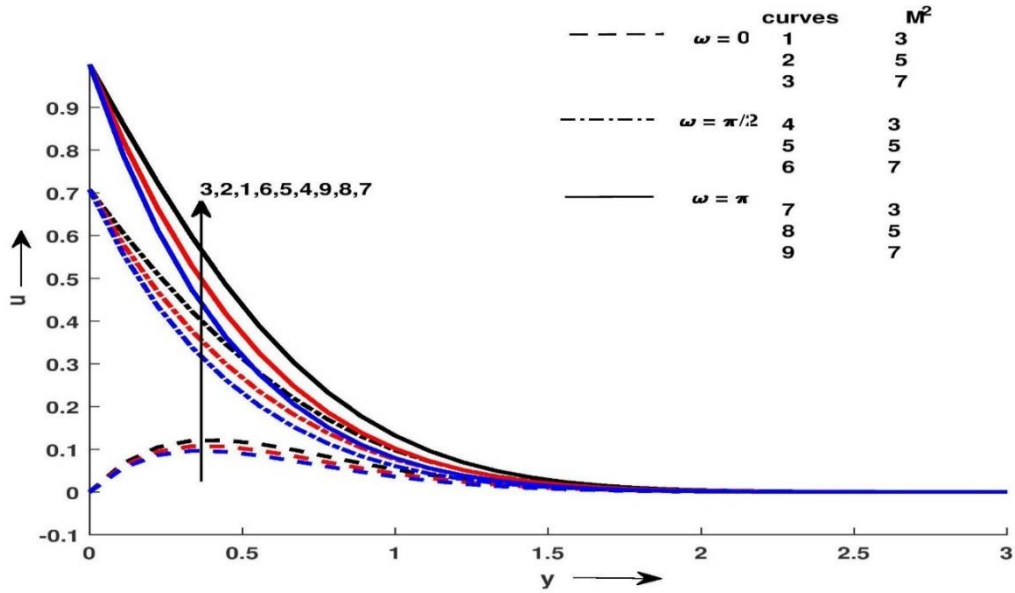

Figure 2.3: Velocity profile for y and M at $t = 0.5,\ Gr = 5,\ \emptyset = 0.03,$ $Pr = 6.2, Nr = 0.5$

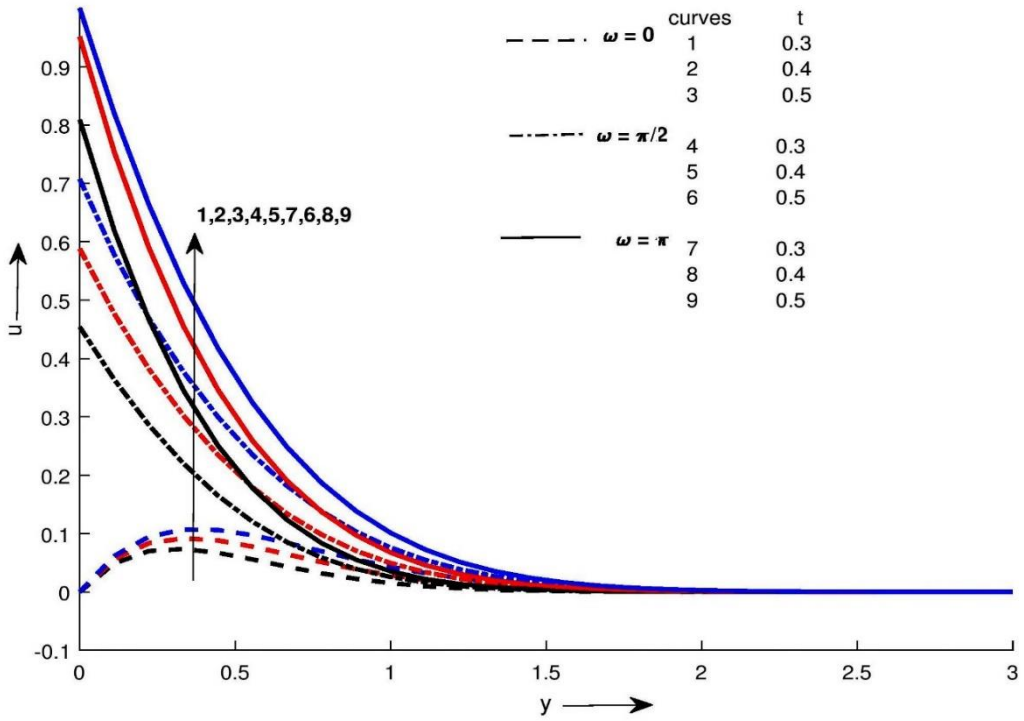

Figure 2.4: Velocity profile for y and t at $M = 3,\ Gr = 5,\ \emptyset = 0.03,$ $Pr = 6.2,\ Nr = 0.5$

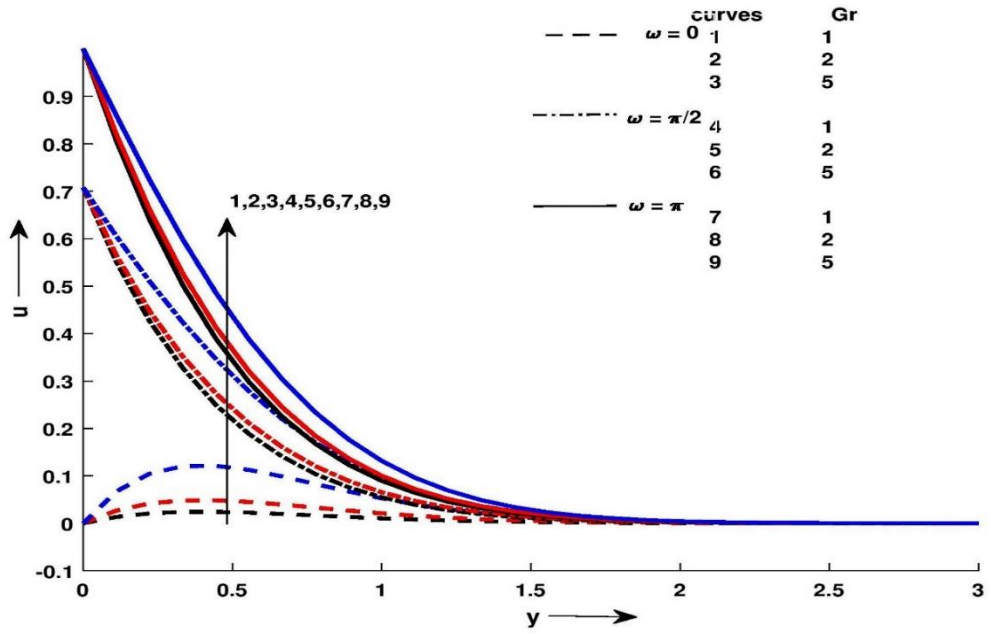

Figure 2.5: Velocity profile for y and Gr at $M = 3,\ t = 0.5,$ $\emptyset = 0.03,\ Pr = 6.2, Nr = 0.5$

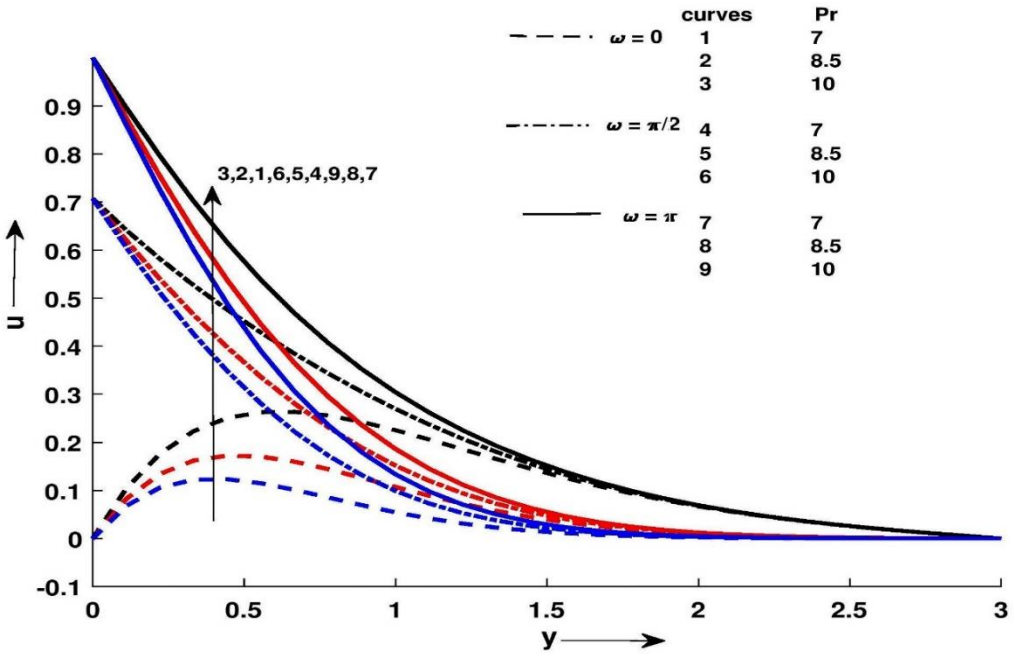

Figure 2.6: Velocity profile for y and Pr at $M = 3,\ t = 0.5,\ \emptyset = 0.03,$ $Gr = 5,\ Nr = 0.5$

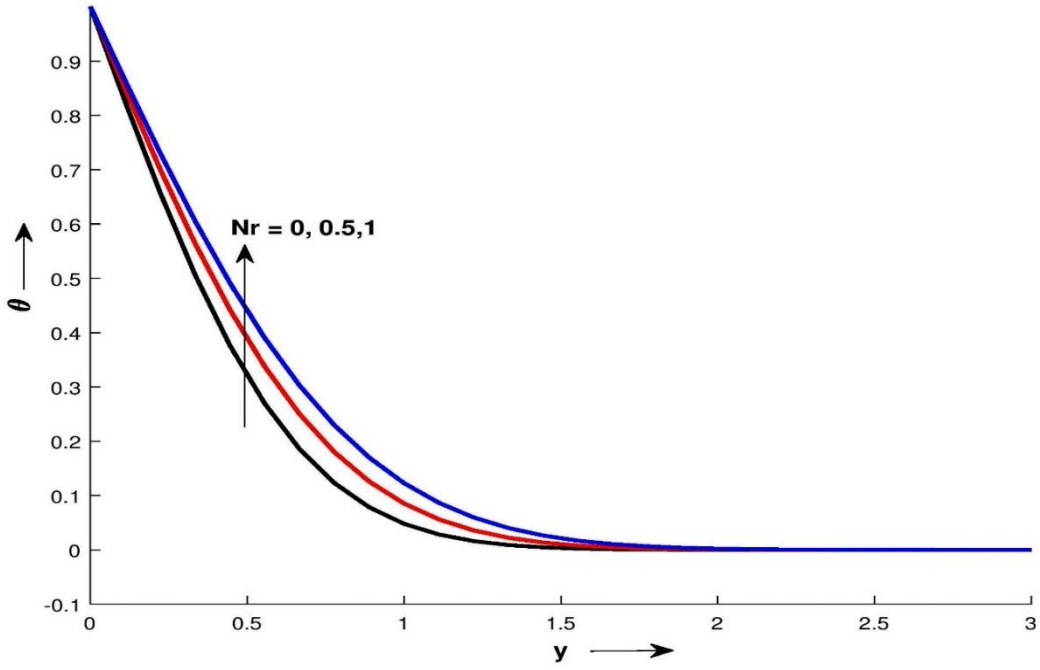

Figure 2.7: Temperature profile for y and Nr at $M = 3,\ t = 0.5,$ $\emptyset = 0.03,\ Gr = 5,\ Pr = 6.2$

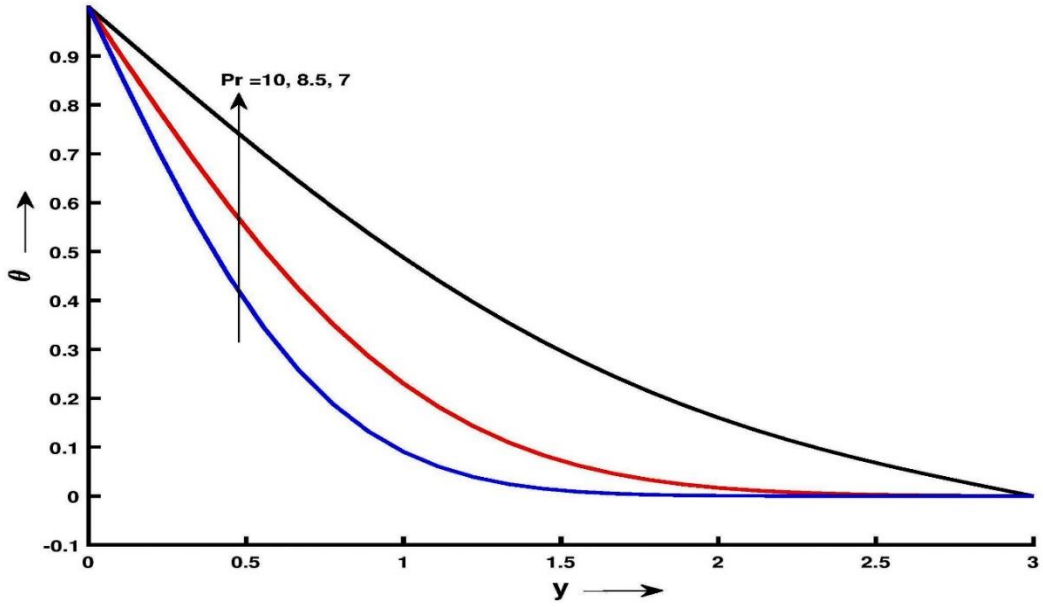

Figure 2.8: Temperature profile for y and Pr at $M = 3, t = 0.5,$ $\emptyset = 0.03,\ Gr = 5,\ Nr = 0.5$

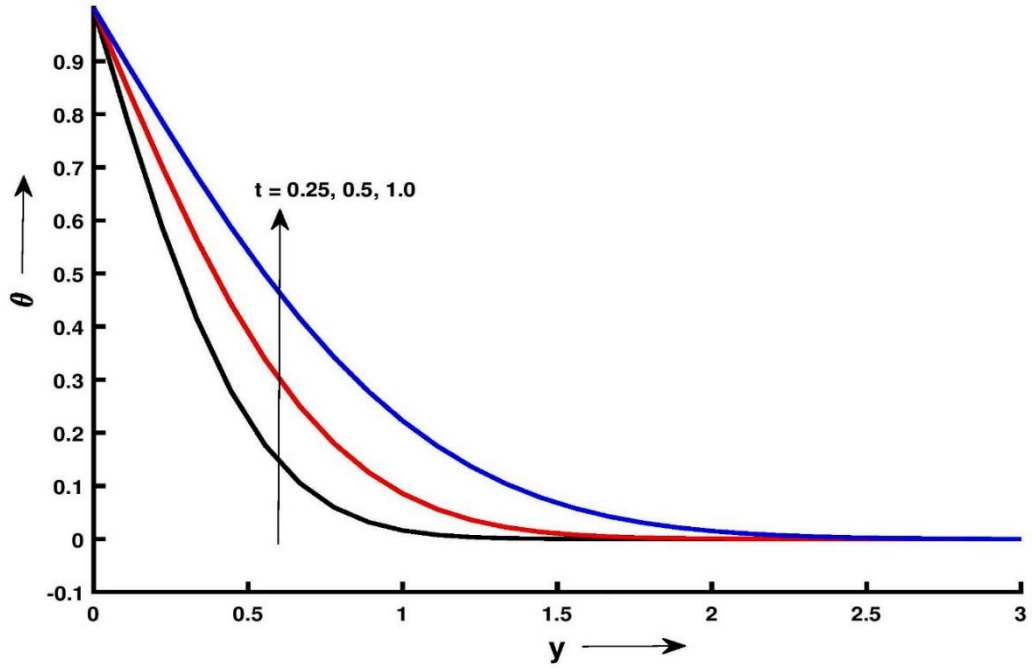

Figure 2.9: Temperature profile for y and t at $M = 3, Nr = 0.5,$ $\emptyset = 0.03,\ Gr = 5,\ Pr = 6.2$

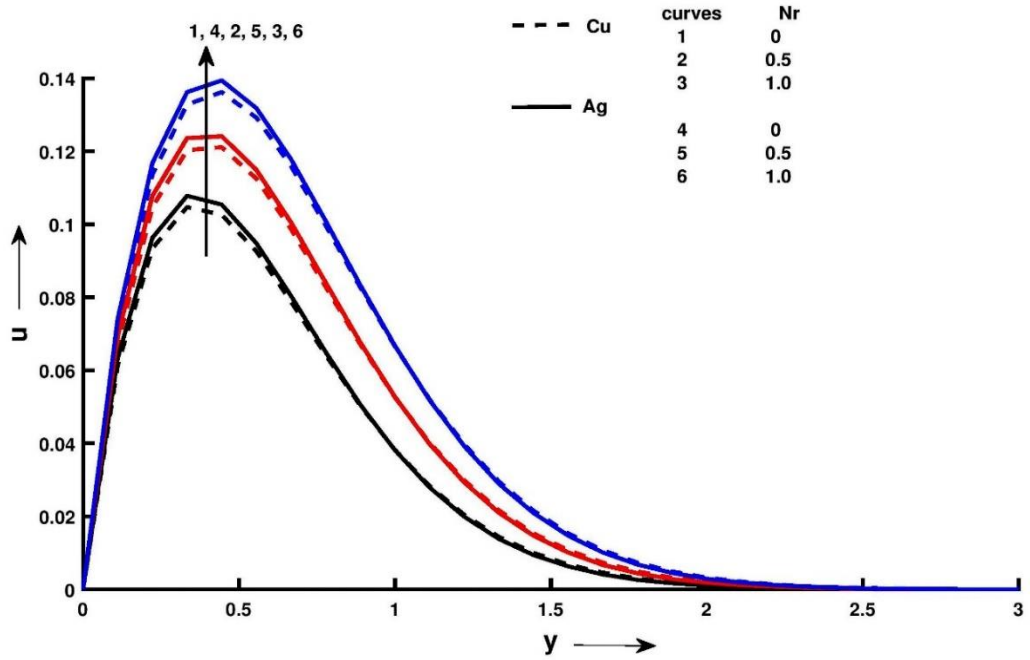

Figure 2.10: Velocity profile for different Nanofluids and Nr at $M = 3, t = 0.5,$ $\emptyset = 0.03, Gr = 5, Pr = 6.2, \omega = 0.$

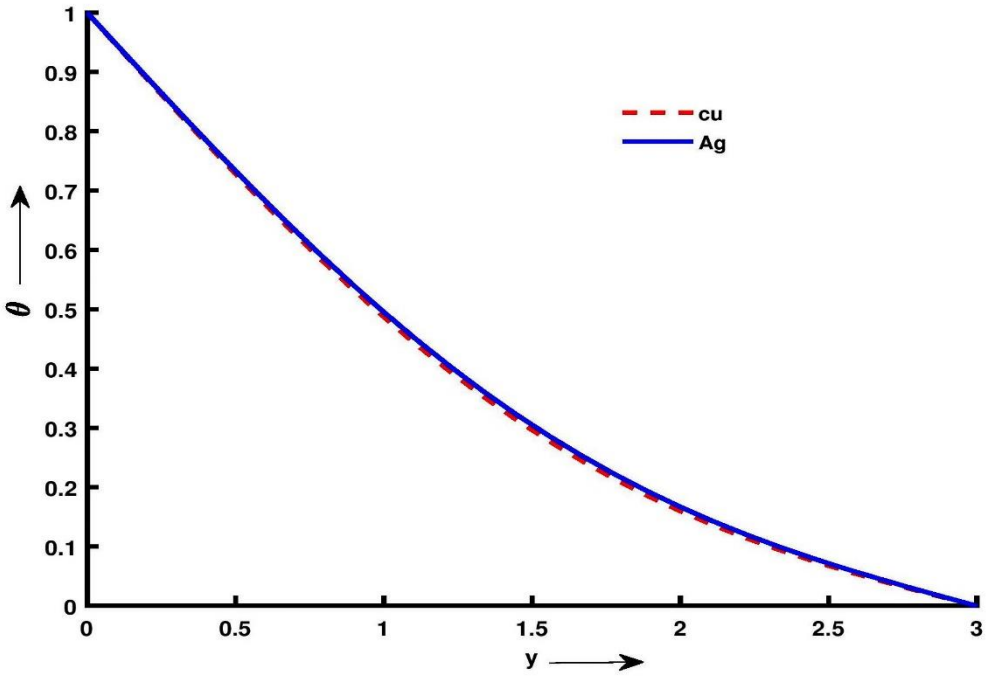

Figure 2.11: Temperature profile for different Nanofluids at $Nr = 0.5, M = 3,$ $t = 0.5, \emptyset = 0.03,\ Gr = 5,\ Pr = 6.2,\ \omega = 0$

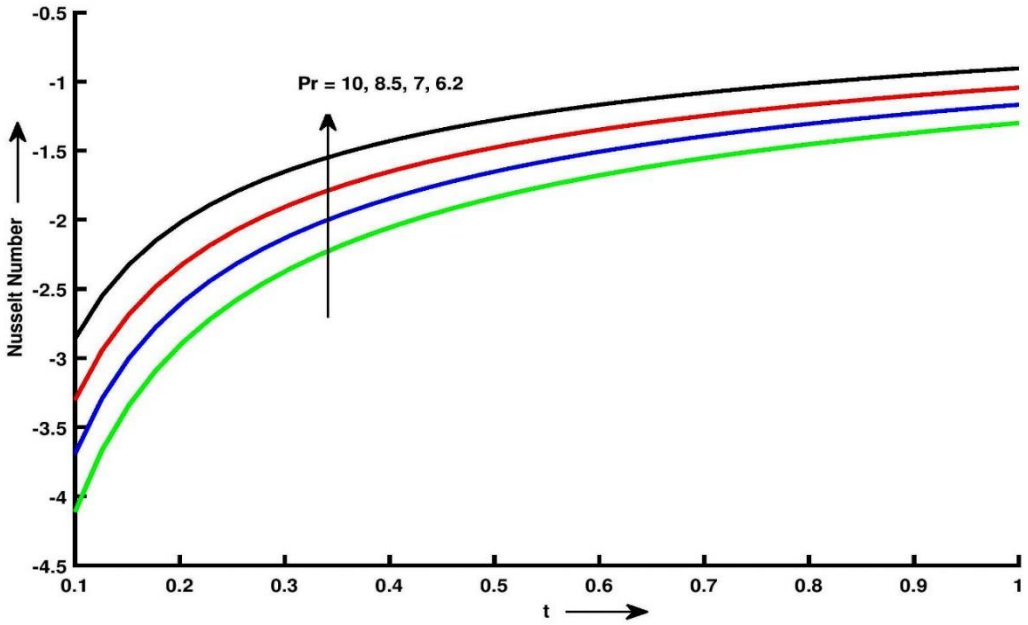

Figure 2.12: Nusselt number for Pr and t at $M = 3,\ \emptyset = 0.03, Gr = 5,$ $Nr = 0, \omega = 0.$

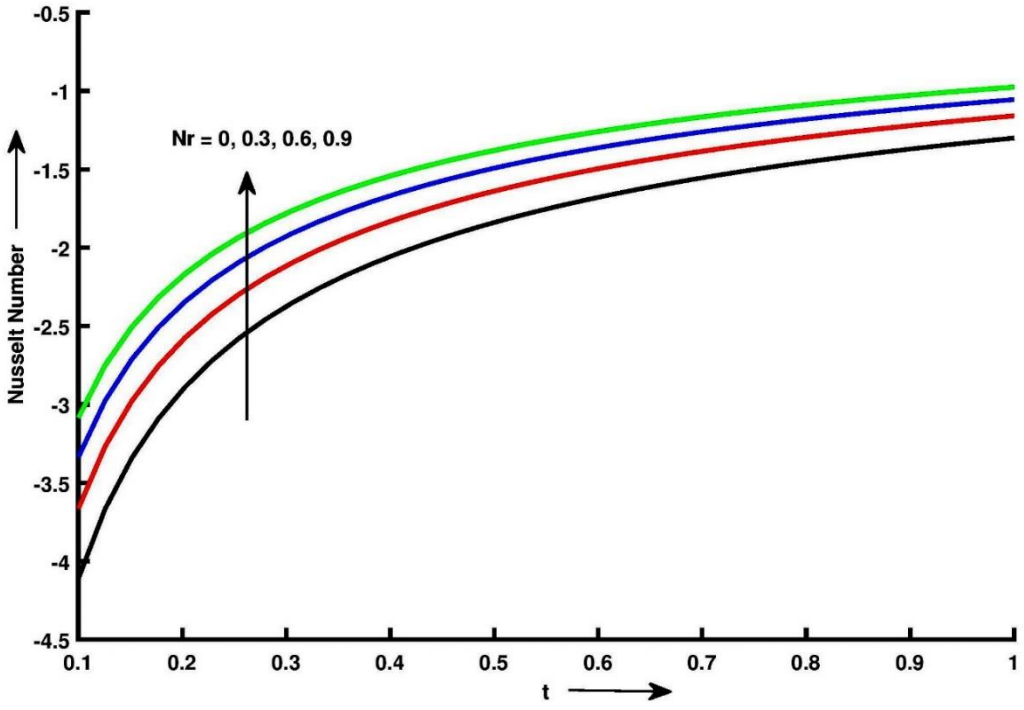

Figure 2.13: Nusselt number for Nr and t at $M = 3,\ \emptyset = 0.03,\ Gr = 5,$ $Pr = 6.2, \omega = 0.$

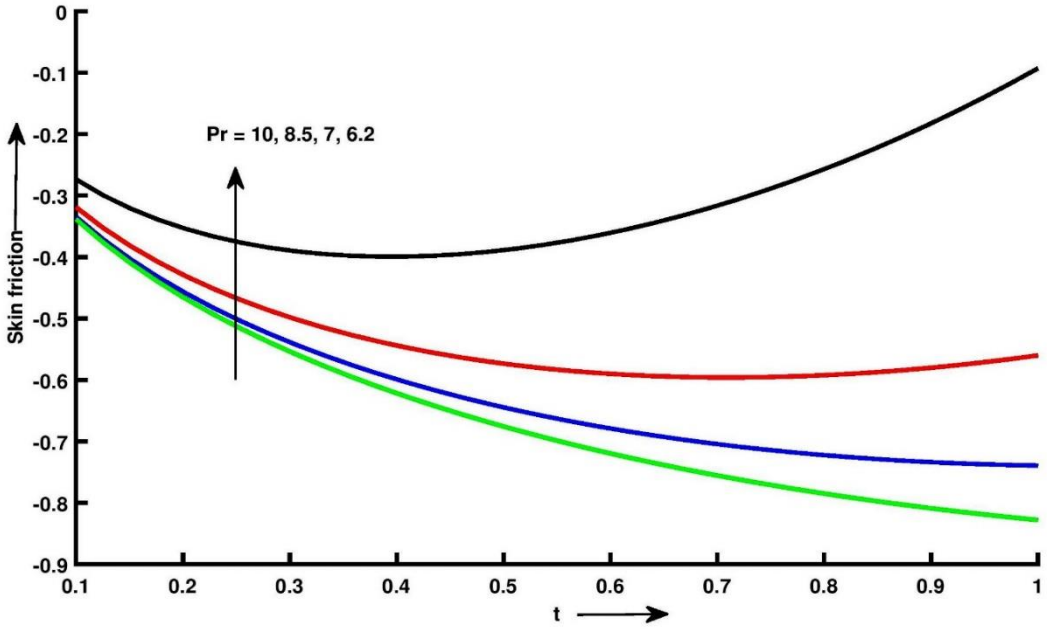

Figure 2.14: Skin friction for Pr and t at $M = 3,\ \emptyset = 0.03,$

$Gr = 5, Nr = 0, \omega = 0$

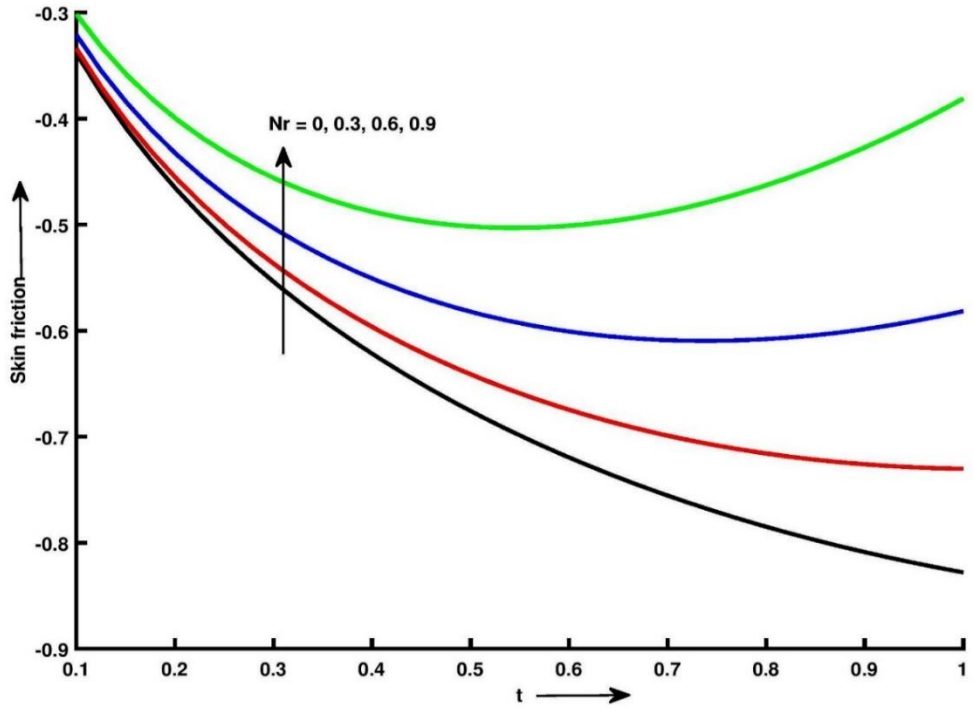

Figure 2.15: Skin friction for Nr and t at $M = 3,\ \emptyset = 0.03,$

$Gr = 5,\ Pr = 6.2, \omega = 0$

Figure 2.2 represents velocity profile for different values of Nr and ω keeping other parameters fixed. It is observed that the fluid velocity u increases with radiation parameter Nr for different values of ω. The velocity increases steeply near the surface of the plate and after attaining the maximum value, the curve settle down to the corresponding asymptotic value for $\omega = 0$ while for other values of ω, velocity decreases as it goes far from plate. Figure 2.3 shows the effect of magnetic parameter M on the velocity. It is seen that the amplitude of the velocity as well as the boundary layer thickness decreases when M is increased. Physically, it may be due to the fact that the application of a transverse magnetic field results in Lorentz force similar to the drag force, and upon increasing the values of M, the drag force increases which leads to the deceleration of the flow. Figure 2.4 reveals the influence of dimensionless time t on the velocity profile. It is found that the velocity is an increasing function of time t. Figure 2.5 depicts the profile of velocity for different values of Grashof number Gr. It is observed that velocity increases with increasing values of Gr. The flow is accelerated due to the enhancement in the buoyancy forces corresponding to increasing values of Grashof number, i.e. free convection effects. Figure 2.6 exhibits the velocity profile for different values of Prandtl number Pr, when the other parameters are fixed. It is observed that velocity of the fluid decreases with increasing Prandtl number. Figure 2.7 reveals the effect of radiation parameter Nr on the temperature profile. Temperature increases with increase in radiation parameter as heat energy from the flow region is also increased, resulting in increase in fluid temperature. Similarly, decrease in the values of Nr results in decrease in the Rosseland radiation absorptivity resulting divergence of the radiative heat flux. This escalates rate of radiative heat transfer to the fluid and hence the fluid temperature increases. Figure 2.8 depicts the variation of nanofluid temperature for Prandtl number Pr. The temperature profile exhibits that fluid temperature decreases as Pr increases. This may be due to the fact that higher Pr means relatively low thermal

conductivity, which reduces conduction and as a result, temperature decreases. Figure 2.9 is plotted to show the effects of the dimensionless time t on the temperature profile. Obviously, the temperature increases with increasing time t. This graphical behaviour of temperature is in good agreement with the corresponding boundary conditions of temperature profile as shown in Equation (2.12). Fluid temperature is high near the plate and decreases asymptotically to the free stream with zero value far away from the plate. Figure 2.10 and Figure 2.11 reveal velocity and fluid temperature variations for two types of water based nanofluids Cu – water and Ag – water for different values of Nr. Velocity of silver water nanofluid is more than copper water nanofluid, it is obvious that the velocity distributions for Cu – water and Ag – water are almost the same as their densities are near to each other. However, due to higher thermal conductivity of Ag – water nanofluid, temperature of Ag – water nanofluid is found to be higher than Cu – water. It is also seen that the thermal boundary layer thickness is more for Ag – water than Cu – water nanofluid. Figure 2.12 and Figure 2.13 illustrate effects of Prandtl number Pr and radiation parameter Nr on Nusselt number Nu. Temperature gradient increases with thermal radiation resulting in increased Nu. Increase in Pr results in lower thermal conductivity and thus there is decrease in Nu. Figure 2.14 and Figure 2.15 reveal effects of Prandtl number Pr and radiation parameter Nr on skin friction C_f. Skin friction on plate decreases with increase in Pr while increases with increase in Nr.

Table 2.1 shows effects of Magnetic parameter M, Grashof number Gr, Nanoparticle volume fraction $\emptyset$ on Skin friction C_f and Nusselt number Nu. Negative values of Nu show that heat flows from fluid to plate and that of skin friction reveals exertion of drag force. It is observed that Nu increase with $\emptyset$ as volume fraction of nanoparticle increases thermal conductivity. Nu also increases with time. C_f decreases with increase in Gr as raise in buoyancy accelerates the fluid flow. C_f is a decreasing function of time.

Table 2.1: Skin friction and Nusselt number variation at Pr = 6.2 and Nr = 0.5

t	M	Gr	$\emptyset$	C_f	Nu
0.4	1.1	5	0.05	-0.6196	-1.7179
0.4	1.2	5	0.05	-0.6081	-1.7179
0.4	1.5	5	0.05	-0.5680	-1.7179
0.4	1.5	5.5	0.05	-0.6248	-1.7179
0.4	1.5	6.0	0.05	-0.6816	-1.7179
0.4	1.5	5	0.1	-0.4064	-1.6268
0.4	1.5	5	0.15	-0.2799	-1.5397
0.5	1.5	5	0.05	-0.6043	-1.5366
0.6	1.5	5	0.05	-0.6284	-1.4027

2.8 Conclusions

In this chapter, an exact analysis is performed to investigate effects of radiation, magnetic parameter and various physical parameters on an unsteady MHD flow of an optically thick nanofluid past an oscillating vertical plate. The dimensionless governing equations are solved using the Laplace transform. Water based nanofluid is considered having nanoparticles: copper and silver. The results for velocity and temperature are obtained and plotted graphically.

The main conclusions of this study are:

- The velocity of the nanofluid increases with increase in the radiation parameter Nr for different frequencies of oscillation ω of the plate.
- The velocity of the nanofluid decreases with increase in the magnetic field.
- The Velocity increases with increase in Gr and t.

- Temperature of nanofluid increases with increase in the radiation parameter Nr.
- The temperature of the nanofluid increases with time t.
- Both velocity and temperature of the nanofluid decrease as Prandtl number Pr increases.
- Temperature of Silver-water nanofluid is more compared to Copper-water nanofluid.
- Skin friction and Nusselt number decrease with increase in Prandtl number Pr.
- Skin friction and Nusselt number increase with increase in Radiation Parameter Nr.